sciendo

PRODUCTION ENGINEERING ARCHIVES 2021, 27(2), 124-129

PRODUCTION ENGINEERING ARCHIVES

ISSN 2353-5156 (print)
ISSN2353-7779 (online)

Exist since 4th quarter 2013
Available online at www.pea-journal.eu

The effect of changing graphitization temperature toward bio-graphite from Palm Kernel Shell

Rapidah Othman[1], Afiqah Samsul Kamal[1], N.H. Jabarullah[2]

[1] Department of Chemical Engineering Section, Universiti Kuala Lumpur Malaysian Institute of Chemical and Bioengineering Technology (UniKL MICET), Lot 1988 Vendor City, Taboh Naning, 78000 Alor Gajah, Melaka, Malaysia
[2] Universiti Kuala Lumpur Malaysian Institute of Aviation Technology, Malaysia
Corresponding author e-mail: nhafidzah@unikl.edu.my

Article history
Received 04.03.2021
Accepted 10.05.2021
Available online 14.06.2021

Keywords
Production of Graphite
Graphitic carbon material
Quality of graphite

Abstract
This paper focuses on the relationship between heat treatment temperature toward structural transformation from amorphous carbon to highly graphitic carbon material during a production stage.The following report discusses a simple strategy to convert the palm kernel shell (PKS) into highly crystalline, high quality graphite via simple two-step process. The production involves impregnation of catalyst followed by thermal treatment. Both XRD and Raman spectroscopy allowed the observation of microstructural change of the prepared sample at temperature ranging from 1000°C to 1400°C using Ferum catalyst. From XRD pattern it can be observed that as graphitization temperature increased, the degree of graphitization also increased. Overall sample prepared at higher temperature 1400°C shows a higher degree of graphitization. PKS sample graphitized at 1400°C with the aid of Ferum catalyst shows a sharp intensified peak at $2\theta = 26.5°$ reflecting formation of highly crystalline graphite structure. Raman spectrum also suggests similar results to XRD in which PKS-1400 shows the presence of large amount of graphitic structure as the value of (Id/Ig) ratio is lower than in other samples. HRTEM analysis visibly shows define lattice fringe, which further confirms the structural transformation from amorphous to highly ordered graphitic carbon structure. Overall, good quality graphitic carbon structure from Palm Kernel shell was succesfully synthesised via utilization of PKS, Ferum catalsyt and heat treatment method.

DOI: 10.30657/pea.2021.27.16 JEL: L69, M11

1. Introduction

Graphite is naturally occurring polymorph of crystalline carbon, composed of graphene layer stacked in 3D crystalline lattice (Kalyoncu, 2000; King, 2006; Chehreh Chelgani et al., 2016; Banek et al., 2018). It has received considerable attention in wide range of application due to its diverse properties, such as high thermal conductivity, high melting point, good conductor, and good chemical resistance (Nettelroth et al., 2016). Having both metal and non-metal properties make it suitable to be used in a wide range of industrial applications, including aluminium industries, lubricants, refractories, electrical products, pencil, and precursor for graphene production (Kalyoncu, 2000; Chehreh Chelgani et al., 2016; Samsul, Othman and Jabarullah, 2020).

Synthetic graphite is a man-made substance manufactured by high temperature process, arc discharge, laser ablation, and chemical vapor deposition (Albert and Mills Inc, 2006; Lovás et al., 2011; Shi et al., 2016; Banek et al., 2018; Thambiliyagodage et al., 2018). Heat treatment process usually done by using coke and coal tar pitch as carbon precursor (Albert and Mills Inc, 2006; Banek et al., 2018). This conventional pathway, however, is energy-consuming, costly and not environmentally friendly (Kim, Lee and Lee, 2016; Banek et al., 2018; Fromm et al., 2018). Thus, catalytic graphitization using lignocellulosic waste as carbon precursor has become a great option, as it is a cost effective, uncomplicated, and reliable method (Käärik et al., 2008; Sultana et al., 2019).

Catalytic graphitization is the process of transforming non-graphitic carbon to graphitic carbon structure by heat treatment in the present of certain metal or mineral (Gutiérrez-Pardo et al., 2015; Radzyminska-Lenarcik, Ulewicz and Ulewicz, 2018). Catalytic graphitization using transition metals, such as Fe, Co ,Ni, Mg or metalloid element has been

widely reported as an effective approach for the structural transformation from amorphous carbon to graphitic carbon material (McKee, 1973; Sevilla and Fuertes, 2010; Liu et al., 2013; Gutiérrez-Pardo et al., 2015; Khokhlova et al., 2015; Thompson et al., 2015). Iron is one of the most widely used catalysts, and was found to be the most effective catalyst for graphite production (Hoekstra et al., 2015, 2016; Thompson et al., 2015; Nettelroth et al., 2016; Shi et al., 2016).

In catalytic graphitization process, numbers of process parameter play an important role in determining the structure and quality of graphitic carbon produce (Demir et al., 2015; Gutiérrez-Pardo et al., 2015; Hoekstra et al., 2016; Nettelroth et al., 2016; Gupta et al., 2017; Ishchuk, Sozanskyy and Pukała, 2020) Graphitization can be done at various range of temperature, various amount of catalyst loading, different type of catalyst and various type of carbon precursor with addition of pre-treatment or activating agent depending on desired end product (M. T. T. Johnson and Faber, 2011; Gutiérrez-Pardo et al., 2015; Hou et al., 2019).

Type of carbon precursor is one of important process parameter in graphite production. Generally, carbon rich material such as coke and coal tar pitch are utilized (Lisiecka et al., 2018). However, contemporary research has been shifted toward greener and sustainable option, such as biomass waste (Paun et al., 2016; Slovaca and Cehl, 2016). Oil palm is among important commodities in Malaysia but it has led to a huge amount of biomass waste (Jabarullah, 2016; Dungani et al., 2018). The waste comprises of Palm Kernel Shell (PKS), Empty Fruit Bunch (EFB), and Palm Mesocarp Fiber yearly (PMF) (Dalton, Mohamed and Chikere, 2017; Ma et al., 2017). Generally, oil palm waste is a good source of biomaterial, it has received great attention due to its potential to be utilized in wide range of application, (Dungani et al., 2018). It is a material naturally rich in carbon . Production of carbon material from biomass waste will reduce enviromental problems and maximize the utilization (Cioca and Cioc, 2010; Pacana and Ulewicz, 2017; Xia et al., 2018)

Actions should be taken due to a need to utilize the oil palm waste based on the technological aspect, cost-effectiveness, the balance of energy consideration of the environmental effect as the solution for the problem (Rada and Cioca, 2017; Rada et al., 2018). It is, therefore, vital to create an experiment which would take advantage of green waste generated by oil palm industries (Kučerová et al., 2015). The utilization of useful waste can be seen as a step towards zero-waste industry.

Therefore, this work demonstrates simple 2-step process for graphite production using Palm kernel shell (PKS) by heat treatment ranging from 1000˚C to 1400˚C with present of Iron catalyst. As heat treatment plays an important role in supplying the energy for macromolecules rearrangement during catalytic graphitization process, this process' parameter is further discussed within this research work (M. T. T. Johnson and Faber, 2011). This research work will give an insight into one of important parameters for catalytic graphitization, as there is no previous literature discuss on utilization of palm oil waste as carbon precursor.

2. Experimental

Palm Kernel shell waste collected from Bell KSL Sawit Sdn. Bhd-first underwent drying process under direct sunlight for 24 hours to remove moisture content. The raw material was then rinsed with distilled water to remove impurities. The sample was next oven dried at 70˚C for 24 -hour duration to remove excess water content. In the next step, the sample was grinded using Golden Bull 1.2 kW Universal Powder Mill SY-116 and sieved to achieve constant size 206μm.

The sample It was subsequently carbonized in the Carbolite 1800C Tube Furnace / Model CTF 18/300. The carbonization temperature was set at 500˚C at ramping rate 5˚C/min with 30 ml/min constant nitrogen flow throughout the process and 60-minute isotherm 500˚C. After carbonization, catalyst impregnation process were prepared by mixing 5g of carbonized Palm Kernel shell powder with 100 ml Iron (III) Nitrate solution (60%, 12.98 g) under vigorous stirring. It was then transferred to round bottom flask and refluxed for 5h. The solid was then filtered and dried.

Next, 2g of dried sample was placed in quartz holder and graphitize in Carbolite 1800C Tube Furnace / Model CTF 18/30 under nitrogen atmosphere at temperature ranging from 1000˚C to 1400˚C at rate of 5˚C /min and 120-minute isotherm. The palm kernel shell sample prepared at different graphitizing temperature were denoted as PKS-1000, PKS -1100, PKS-1200, PKS-1300 and PKS-1400. After graphitization, the residual catalyst was removed by stirring it with 1M HCl for 24 hours, followed by washing with deionized water and dried in the oven at 80˚C overnight.

To identify the crystalline material, X-ray diffraction analysis (XRD) are commonly used probe. In this research PANanalytic X'Pert Pro diffractometer using Cu Kα radiation (λ=1.5406 Å, 45 kV, 35 mA) in 2-theta range of 2 to 90 degree, at step size 0.02˚ radiation is use for data collection. Raman spectra were recorded using a Renishaw Micro-Raman system 2000 with He-Ne laser excitation λ= 632 nm. HRTEM images analysis were performed using FEI Tecnai G2 20 S-twin transmission electron microscope ((HR)TEM, FEI), operated at 200 kV equipped with a filed-emission gun supplied image at atomic level. The sample were prepared by sonicated in ethanol for 10 minutes, deposited into HRTEM grids.

3. Results and discussion

Heating temperature was among the important factor that control the quality of graphitic carbon material. This study revealed trends on how this factor influences degree of graphitization.The influence of graphitization temperature was first determined based on XRD pattern. Fig.1 shows the XRD patterns for all PKS sample prepared at various graphitization temperature. All carbon sample exhibits well resolved (002) diffraction peak at 2Θ= 26˚corresponding to (002) plane of graphite (Chen et al., 2018; Made Joni et al., 2018).The patterns clearly exhibit stronger intensified peak as graphitization temperature increased from 1000˚C to 1400˚C associated with strong degree of graphitization. At 1000˚C

only small graphite peak is observed, but, as with temperature increase, the peak is more noticeable.

A similar trend has been reported by M.T. Johnson and Faber, (2011) and Chen et al., (2018) in their research work, diffraction peak with increased kurtosis showing that greater crystalline ordering was achieved at higher heat treatment temperature. Furthermore, a sample prepared at 1400˚C also exhibits noticeable peak at 2Θ~ 42˚, 44˚ and 54˚ corresponding to (100), (101) and (004) diffraction of graphitic frameworks, indicating a better quality in stacking, crystallinity and stacking thickness(Vázquez-Santos et al., 2012; Made Joni et al., 2018).

For comparison from Fig. 2, control PKS sample, that was prepared at 1400˚C without addition of any catalyst shows almost no reflection peak. This suggest that the absent of catalyst hindered the modification of lignocellulosic biomass that initially known as hard carbon material, probably higher energy needed for the transformation without aid of catalyst. PKS-1400 were also compared with commercial graphite; although the peak is not intensified as commercially available graphite, but the present of sharp peak still provides significant information showing successful transformation from amorphous to crystallize graphitic structure.

The value of d_{002} spacing was calculated according to Bragg's equation were summarize in Table 1. The value of d_{002} spacing in range between 0.3319-0.3345 nm, close to the value of 0.3354 nm of pure graphite and less than 0.344nm of amorphous structure. Of all the samples, PKS -1400 (0.3345 nm) showed the nearest to 0.3354 nm corresponding to ideal graphite suggesting that ordered carbon framework was achieved (Vázquez-Santos et al., 2012).

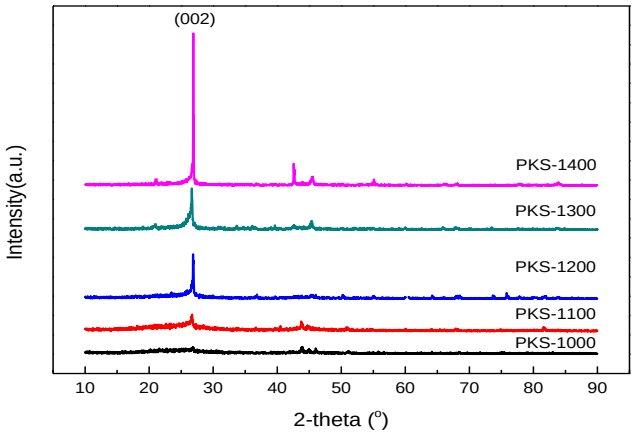

Fig. 1. XRD patterns of graphitic carbon prepared at different graphitization temperature.

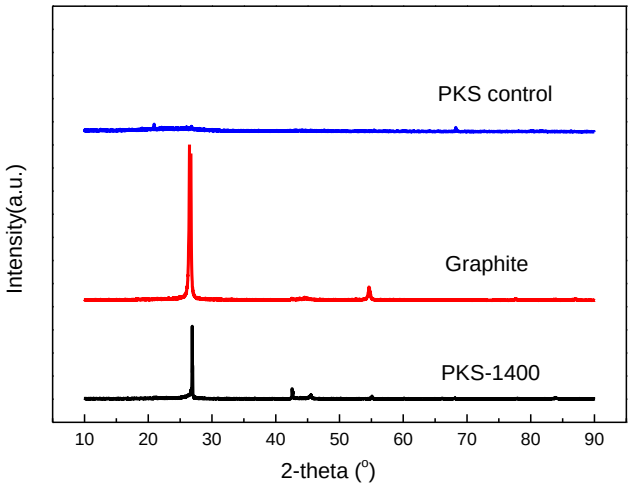

Fig. 2. XRD pattern of PKS-1400, Graphite and PKS control sample

Table 1. Physical properties of bio-graphite**.**

Sample	d_{002} (nm)	I_d/I_g
Graphite	0.33500	0.331
PKS control	0.3316	1.058
PKS-1400	0.3345	0.689
PKS-1300	0.3339	0.777
PKS-1200	0.3319	0.751
PKS-1100	0.3325	0.931
PKS-1000	0.3322	0.958

The effect of heat treatment temperature toward quality of structural organization of graphitic material was further evaluated by Raman Spectroscopy (Sevilla, Sanchís, Valdés-Soh, et al., 2007). Raman spectra for carbon materials consist of four first-order Raman band, each from different vibratory modes. For graphitic carbon material most significant band, was located near 1580 cm^{-1} represent vibration in ideal graphite lattice(G) band (M. T. Johnson and Faber, 2011; Kim, Lee and Lee, 2016; Lim et al., 2017). Meanwhile (D) band appear as increasing in structural defect, D1 (1350cm^{-1}), D2 (1620 cm^{-1}) and D3(1400 cm^{-1}) bands represent vibrations from graphene layer edges, surfaces, and amorphous regions respectively (Major et al., 2018).

Peak intensity ratio of prominent G and D1 bands is an indicator of degree of graphitic material content and quality(M. T. Johnson and Faber, 2011). The relative intensity ratio between D and G bands (I_d/I_g) reflects the degree of graphitization. Lower I_d/I_g value clearly indicates a high degree of graphitization(Sevilla, Sanchís, Valdés-Solís, et al., 2007). PKS-1400, PKS-1300 samples were compared with a commercial graphite.

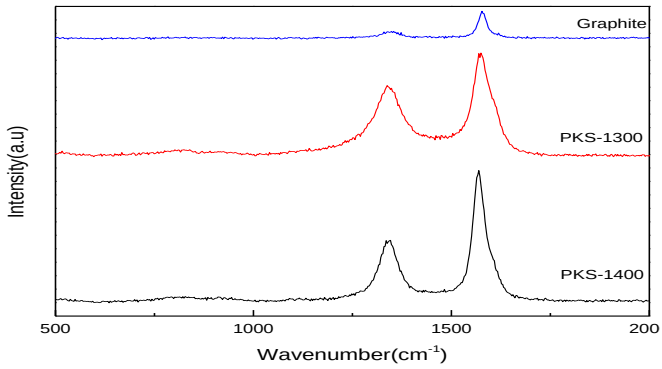

Fig. 3. Raman Spectra of Commercial graphite, PKS-1300 and PKS-1400

As reported in Table 1, the I_d/I_g value for PKS-1400, PKS-1300 and commercial graphite is 0.689,0.777 and 0.311, respectively. The Raman spectra for PKS-1400, PKS-1300 and commercial graphite are displayed in Fig. 3. Lower relative intensity ratio I_d/I_g indirectly proving successful alteration of amorphous material has been achieved with the aid of Iron catalyst. This data proving that sample underwent a thermal treatment at a higher temperature showing high crystallinity and lower defect as I_d/I_g ratio for PKS-1400 is lower among other sample, this result is in coherent with XRD finding. In addition, the control sample prepared without any catalyst shows Id/Ig value of 1.05 related with more defect structure. It proves that catalyst play an important role to help in modifying the carbon structure. Both XRD and Raman analysis have suggested that higher degree of graphitization achieve at higher heat treatment temperature.

Effect of heat treatment temperature might happen due to nucleation of catalyst, as it grow into larger nanoparticle as heating temperature increased (Liu et al., 2013). At higher temperature catalyst particle will quickly grow into particle with considerable size, good crystallinity, and good dispersion that can facilitate formation of shell-like graphitic nanostructure (Samsul, Othman and Jabarullah, 2020). Graphite might be form either by direct precipitation from the catalyst or by the evolution of quasi-graphitic nanostructure through self-ordering process(Liu et al., 2013).

To further confirm the transformation of PKS amorphous structure to highly graphitic carbon structure, a High-Resolution Transmission Electron Microscope (HRTEM) images were performed. PKS control sample Fig. 4 (b) exhibits disordered microstructure typical of amorphous carbon. On the other hand, the PKS 1400 exhibits crystalline ordered structure from Fig. 4 (a), visible set of core lattice fringes with d-spacing of 0.33 nm in a good agreement to d-spacing of (002) of graphitic carbon from XRD data. The HRTEM image in Fig. 4 (a) demonstrates high degree of crystallinity. The estimation of d-spacing is deduce by using Gatan digital micrograph software.

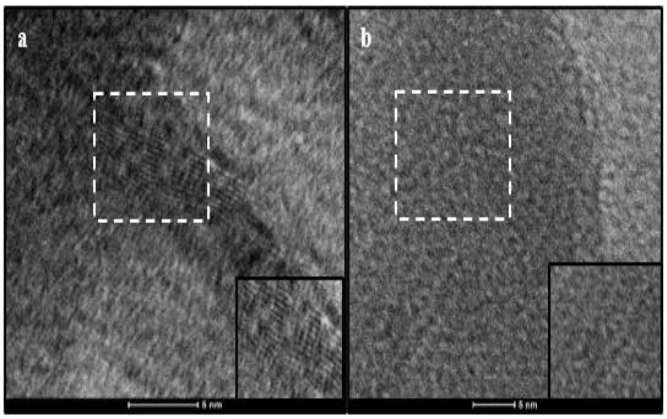

Fig. 4. HRTEM image (a) PRE PKS Fe-1000 (b) PKS control

Referring to HRTEM images, it was further confirmed that the structural transformation of lignocellulosic materials into highly graphitic carbon was successfully achieved. From overall observation it can be deduced that heat treatment temperature play an important role in controlling product quality. So far researcher have agreed that higher heat treatment temperature is still preferable, however further investigation can be made to enhance the quality of graphite produce at lower temperature.

4. Summary and conclusion

The result of this study shows that:

- Graphitic carbon material with high crystallinity have been succesfully synthesize using Palm kernell shell based on XRD and RAMAN analysis.
- Degree of graphitization and quality of graphite can be regulated by changing the temperature. Higher heat treatment temperature 1400˚C responsible higher degree of graphitization.
- XRD data reported 2Θ~26˚ peak appear for all sample, but additional graphite peak is noticeable for PKS prepared at 1300˚C and 1400˚C.
- The value of d_{002} spacing of all sample is close to value 3.354 of pure graphite and less than 3.44 for disorder carbon**,** proving that the production of graphite from lignocellulosic material is promising alternative way.
- Lower Id/Ig ratio can be achieved at higher processing temperature.
- HRTEM image show successful transformation as crystalline graphitic carbon order structure appear in PKS-1400.

Acknowledgements

The research was supported by FRGS grant (Ref: FRGS/1/2015/TK05/UNIKL/02/1) for the funding.

Reference

Albert, T., Mills Inc., 2006. An Introduction to Synthetic Graphite. Introduction to Synthetic Graphite, Available at: https://asbury.com/pdf/SyntheticGraphitePartI.pdf (Accessed: 17 January 2019).

Banek, N.A. et al., 2018. Sustainable Conversion of Lignocellulose to High-Purity, Highly Crystalline Flake Potato Graphite, ACS Sustainable Chemistry and Engineering, 6(10), 13199-13207. DOI: 10.1021/acssuschemeng.8b02799.

Chehreh Chelgani, S. et al., 2016. A Review of Graphite Beneficiation Techniques, Mineral Processing and Extractive Metallurgy Review, 37(1), 58-68, DOI: 10.1080/08827508.2015.1115992.

Chen, C. et al., 2018. Catalytic graphitization of cellulose using nickel as catalyst, BioResources, 13(2), 3165-3176, DOI: 10.15376/biores.13.2.3165-3176.

Cioca, M. and Cioc, L.I., 2010. Decision Support Systems used in Disaster Management, Decision Support Systems, (January), DOI: 10.5772/39452.

Dalton, O.S., Mohamed, A.F., Chikere, A.O., 2017. Status Evaluation of Palm Oil Waste Management Sustainability in Malaysia, OIDA International Journal of Sustainable Development, 10(12), 41-48.

Demir, M. et al., 2015. Graphitic Biocarbon from Metal-Catalyzed Hydrothermal Carbonization of Lignin, Industrial & Engineering Chemistry Research, 54(43), 10731-10739, DOI: 10.1021/acs.iecr.5b02614.

Dungani, R. et al., 2018. Biomaterial from Oil Palm Waste: Properties, Characterization and Applications, Palm Oil, DOI: 10.5772/intechopen.76412.

Fromm, O. et al., 2018. Carbons from biomass precursors as anode materials for lithium ion batteries: New insights into carbonization and graphitization behavior and into their correlation to electrochemical performance, Carbon, Elsevier Ltd, 128, 147-163, DOI: 10.1016/j.carbon.2017.11.065.

Gupta, A. et al., 2017. Effect of graphitization temperature on structure and electrical conductivity of poly-acrylonitrile based carbon fibers, Diamond and Related Materials, Elsevier, 78, 31-38, DOI: 10.1016/J.DIAMOND.2017.07.006.

Gutiérrez-Pardo, A. et al., 2015. Effect of catalytic graphitization on the electrochemical behavior of wood derived carbons for use in supercapacitors, Journal of Power Sources, 278, 18-26, DOI: 10.1016/j.jpowsour.2014.12.030.

Hoekstra, J. et al., 2015. Base metal catalyzed graphitization of cellulose: A combined Raman spectroscopy, temperature-dependent X-ray diffraction and high-resolution transmission electron microscopy study, Journal of Physical Chemistry C, 119(19), 10653-10661, DOI: 10.1021/acs.jpcc.5b00477.

Hoekstra, J. et al., 2016. The effect of iron catalyzed graphitization on the textural properties of carbonized cellulose: Magnetically separable graphitic carbon bodies for catalysis and remediation, Carbon, Elsevier Ltd, 107, 248-260, DOI: 10.1016/j.carbon.2016.05.065.

Hou, L. et al., 2019. Hierarchically porous and heteroatom self-doped graphitic biomass carbon for supercapacitors, Journal of Colloid and Interface Science, Elsevier Inc., 540, 88-96, DOI: 10.1016/j.jcis.2018.12.029.

Ishchuk, S., Sozanskyy, L., Pukała, R., 2020. Optimisation of the relationship between structural parameters of the processing industry as a way to increase its efficiency, Engineering Management in Production and Services, 12(2), 7-20, DOI: 10.2478/emj-2020-0008.

Jabarullah, N.H., 2016. The controversy of biofuel versus fossil fuel, International Journal of Advanced and Applied Sciences, 3(2), 11-14.

Johnson, M.T., Faber, K.T., 2011, Catalytic graphitization of three-dimensional wood-derived porous scaffolds, Journal of Materials Research, 26(01), 18-25, DOI: 10.1557/jmr.2010.88.

Johnson, M.T.T., Faber, K.T.T., 2011. Catalytic graphitization of three-dimensional wood-derived porous scaffolds, Journal of Materials Research, 26(01), 18-25, DOI: 10.1557/jmr.2010.88.

Käärik, M. et al., 2008. The effect of graphitization catalyst on the structure and porosity of SiC derived carbons, Carbon, 46(12), 1579-1587, DOI: 10.1016/j.carbon.2008.07.003.

Kalyoncu, R.S., 2000. Graphite, U.S. Geological Survey Minerals Yearbook Vol . I, Metals & Minerals, 1076.

Khokhlova, G.P. et al., 2015. Effect of heat treatment conditions on the catalytic graphitization of coal-tar pitch, Solid Fuel Chemistry, 49(2), 66-72, DOI: 10.3103/S0361521915020056.

Kim, T., Lee, J., Lee, K.H., 2016. Full graphitization of amorphous carbon by microwave heating †, DOI: 10.1039/c6ra01989g.

King, R.J., 2006. Minerals explained 43: Graphite, in Geology Today. Blackwell Publishing Inc., 71-77.

Kučerová, M. et al., 2015. Eliminating waste in the production process using tools and methods of industrial engineering, Production Engineering Archives, 9, 30-34, DOI: 10.30657/pea.2015.09.08.

Lim, Y. et al., 2017. Increase in graphitization and electrical conductivity of glassy carbon nanowires by rapid thermal annealing, Journal of Alloys and Compounds. Elsevier, 702, 465-471, DOI: 10.1016/J.JALLCOM.2017.01.098.

Lisiecka, B. et al., 2018. Obtaining of biomorphic composites based on carbon materials, Production Engineering Archives, 19(19), 22-25, DOI: 10.30657/pea.2018.19.05.

Liu, Y. et al., 2013. Highly porous graphitic materials prepared by catalytic graphitization, Carbon, 64, 132-140, DOI: 10.1016/j.carbon.2013.07.044.

Lovás, M. et al., 2011. The application of microwave energy in mineral processing - a review, Acta Montanistica Slovaca, 16(2), 137-148.

Ma, Z. et al., 2017. Evolution of the chemical composition, functional group, pore structure and crystallographic structure of bio-char from palm kernel shell pyrolysis under different temperatures, Journal of Analytical and Applied Pyrolysis. Elsevier B.V., 127, 350-359, DOI: 10.1016/j.jaap.2017.07.015.

Made Joni, I. et al., 2018. Augmentation of graphite purity from mineral resources and enhancing % graphitization using microwave irradiation: XRD and Raman studies, Diamond and Related Materials, 88, 129-136, DOI: 10.1016/j.diamond.2018.07.009.

Major, I. et al., 2018. Graphitization of Miscanthus grass biocarbon enhanced by in situ generated FeCo nanoparticles, 20, 2269, DOI: 10.1039/c7gc03457a.

McKee, D.W., 1973. Carbon and Graphite Science, Annual Review of Materials Science, 3(1), 195-231, DOI: 10.1146/annurev.ms.03.080173.001211.

Nettelroth, D. et al., 2016. Catalytic graphitization of ordered mesoporous carbon CMK-3 with iron oxide catalysts: Evaluation of different synthesis pathways, Physica Status Solidi (A) Applications and Materials Science, 213(6), 1395-1402, DOI: 10.1002/pssa.201532796.

Pacana, A., Ulewicz, R., 2017. Research of determinations motiving to implement the environmental management system, Polish Journal of Management Studies, 16(1), 165-174, DOI: 10.17512/pjms.2017.16.1.14.

Paun, V.A. et al., 2016. Liposome loaded chitosan hydrogels, a promising way to reduce the burst effect in drug release a comparativ analysis, Materiale Plastice, 53(4), 590-593.

Rada, E.C. et al., 2018. Circular economy and waste to energy, AIP Conference Proceedings, 1968, DOI: 10.1063/1.5039237.

Rada, E.C., Cioca, L., 2017. Optimizing the Methodology of Characterization of Municipal Solid Waste in EU under a Circular Economy Perspective, Energy Procedia, 119, 72-85, DOI: 10.1016/j.egypro.2017.07.050.

Radzyminska-Lenarcik, E., Ulewicz, R., Ulewicz, M., 2018. Zinc recovery from model and waste solutions using polymer inclusion membranes (PIMs) with 1-octyl-4-methylimidazole, Desalination and Water Treatment, 102 (January 2008), 211-219, DOI: 10.5004/dwt.2018.21826.

Samsul, A., Othman, R., Jabarullah, N.H., 2020. Preparation and synthesis of synthetic graphite from biomass waste : A review, 11(2), 881-894.

Sevilla, M., Sanchís, C., Valdés-Soh, T., et al., 2007. Synthesis of graphitic carbon nanostructures from sawdust and their application as electrocatalyst supports, Journal of Physical Chemistry C, 111(27), 9749-9756, DOI: 10.1021/jp072246x.

Sevilla, M., Sanchís, C., Valdés-Solís, T., et al., 2007. Synthesis of graphitic carbon nanostructures from sawdust and their application as electrocatalyst supports, Journal of Physical Chemistry C, 111(27), 9749-9756, DOI: 10.1021/jp072246x.

Sevilla, M., Fuertes, A.B., 2010. Graphitic carbon nanostructures from cellulose, Chemical Physics Letters. Elsevier B.V., 490(1-3), 63-68, DOI: 10.1016/j.cplett.2010.03.011.

Shi, J. et al., 2016. Synthesis of graphene encapsulated Fe3C in carbon nanotubes from biomass and its catalysis application, Carbon. Elsevier Ltd, 99, 330-337, DOI: 10.1016/j.carbon.2015.12.049.

Slovaca, A.M., Cehl, M., 2016. New approach to the basic evaluation of raw material resources in market economy, Acta Montanistica Slovaca, 6(January), 42-55.
Sultana, K.N. et al., 2019. Synthesis of Graphitic Mesoporous Carbon from Metal Impregnated Silica Template for Proton Exchange Membrane Fuel Cell Application, (1), 27-34, DOI: 10.1002/fuce.201800034.
Thambiliyagodage, C.J. et al., 2018. Catalytic graphitization in nanocast carbon monoliths by iron, cobalt and nickel nanoparticles, Carbon. Elsevier Ltd, 134, 452-463, DOI: 10.1016/j.carbon.2018.04.002.
Thompson, E. et al., 2015. Iron-catalyzed graphitization of biomass, Green Chemistry, Royal Society of Chemistry, 17(1), 551-556, DOI: 10.1039/c4gc01673d.
Vázquez-Santos, M.B. et al., 2012. Comparative XRD, Raman, and TEM study on graphitization of PBO-derived carbon fibers, Journal of Physical Chemistry C, 116(1), 257-268, DOI: 10.1021/jp2084499.
Xia, J. et al., 2018. Three-dimensional porous graphene-like sheets synthesized from biocarbon via low-temperature graphitization for a supercapacitor, Green Chemistry, 20(3), 694-700, DOI: 10.1039/c7gc03426a.

改变石墨化温度对棕榈仁壳对生物石墨的影响

關鍵詞
石墨生产
石墨碳材料
石墨质量

摘要
本文着重研究了热处理温度与生产阶段从无定形碳到高石墨碳材料的结构转变之间的关系。本报告讨论了通过简单的两步过程将棕榈仁壳（PKS）转变为高度结晶的高质量石墨的简单策略。生产涉及催化剂的浸渍，然后进行热处理。XRD 和拉曼光谱都允许使用 Ferum 催化剂在 1000°C 至 1400°C 的温度范围内观察制备的样品的微观结构变化。从 XRD 图可以看出，随着石墨化温度的升高，石墨化的程度也随之提高。在较高温度 1400°C 下制备的总体样品显示出较高的石墨化程度。借助于 Ferum 催化剂在 1400°C 石墨化的 PKS 样品在 2θ=26.5° 处显示出尖锐的增强峰，反映出形成了高度结晶的石墨结构。拉曼光谱还暗示了与 XRD 的一致发现，其中 PKS1400 显示出大量的石墨结构，因为（Id / Ig）比值低于其他样品。HRTEM 分析显示出清晰的晶格条纹， 进一步证实了从无定形到高序石墨碳结构的结构转变。总体而言，通过利用 PKS，Ferum catalsyt 和热处理方法成功地合成了来自棕榈仁壳的优质石墨碳结构。